Supplement of Atmos. Chem. Phys., 22, 8221–8240, 2022
https://doi.org/10.5194/acp-22-8221-2022-supplement

Atmospheric Chemistry and Physics
Open Access

Supplement of

Transport of substantial stratospheric ozone to the surface by a dying typhoon and shallow convection

Zhixiong Chen et al.

Correspondence to: Jane Liu (janejj.liu@utoronto.ca) and Xiushu Qie (qiex@mail.iap.ac.cn)

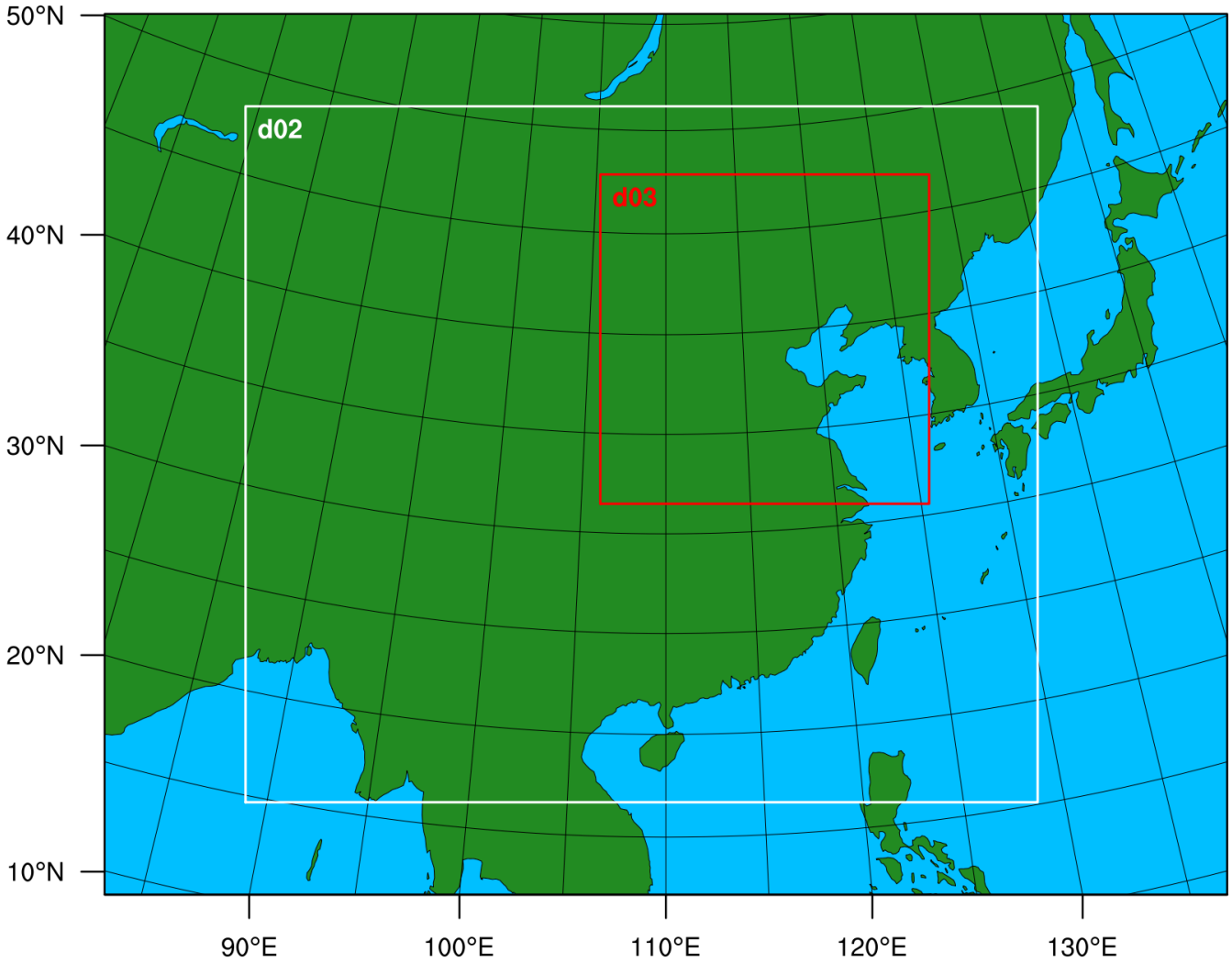

Figure S1: The WRF domains: coarse domain (with horizontal resolution of 27 km) and two nested domains (with horizontal resolution of 9 km and 3 km, respectively)

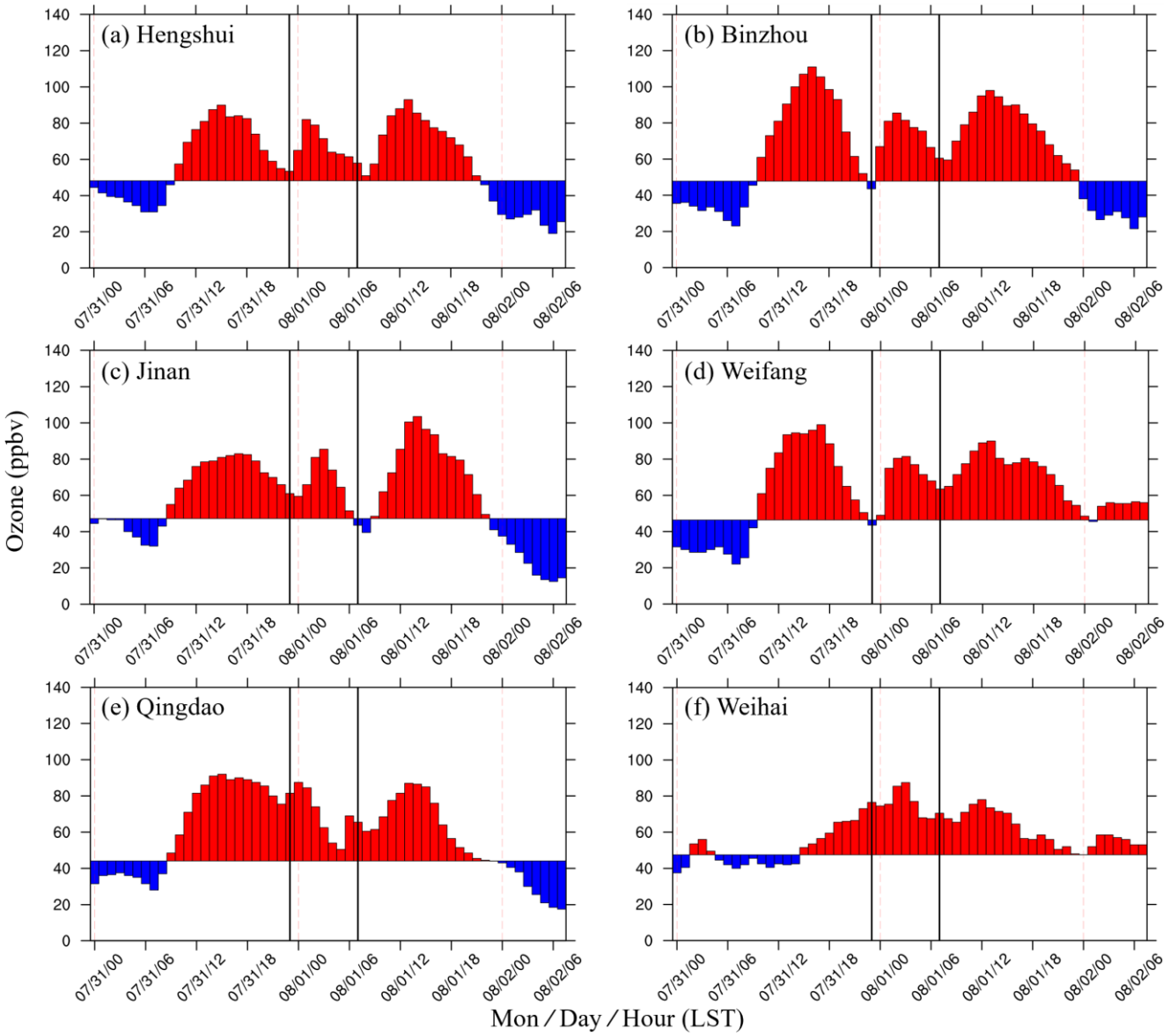

Figure S2: Temporal variation in surface ozone concentrations (unit: ppbv) in local standard time (LST) from 31 July to 02 August 2021 using the 10-day averaged ozone value as a baseline for comparison in cities Hengshui, Binzhou, Jinan, Weifang, Qingdao, and Weihai. Positive (negative) departure from the 10-day averaged ozone concentration is shown in red (blue) color. The two vertical black lines represent the observed ozone surge period between 23:00 LST on 31 July and 06:00 LST on 1 August 2021. Daily cycles (0:00-0:00 LST) are denoted by vertical red lines. Labels along the horizontal axis represent the observation times (mon/day/hour).

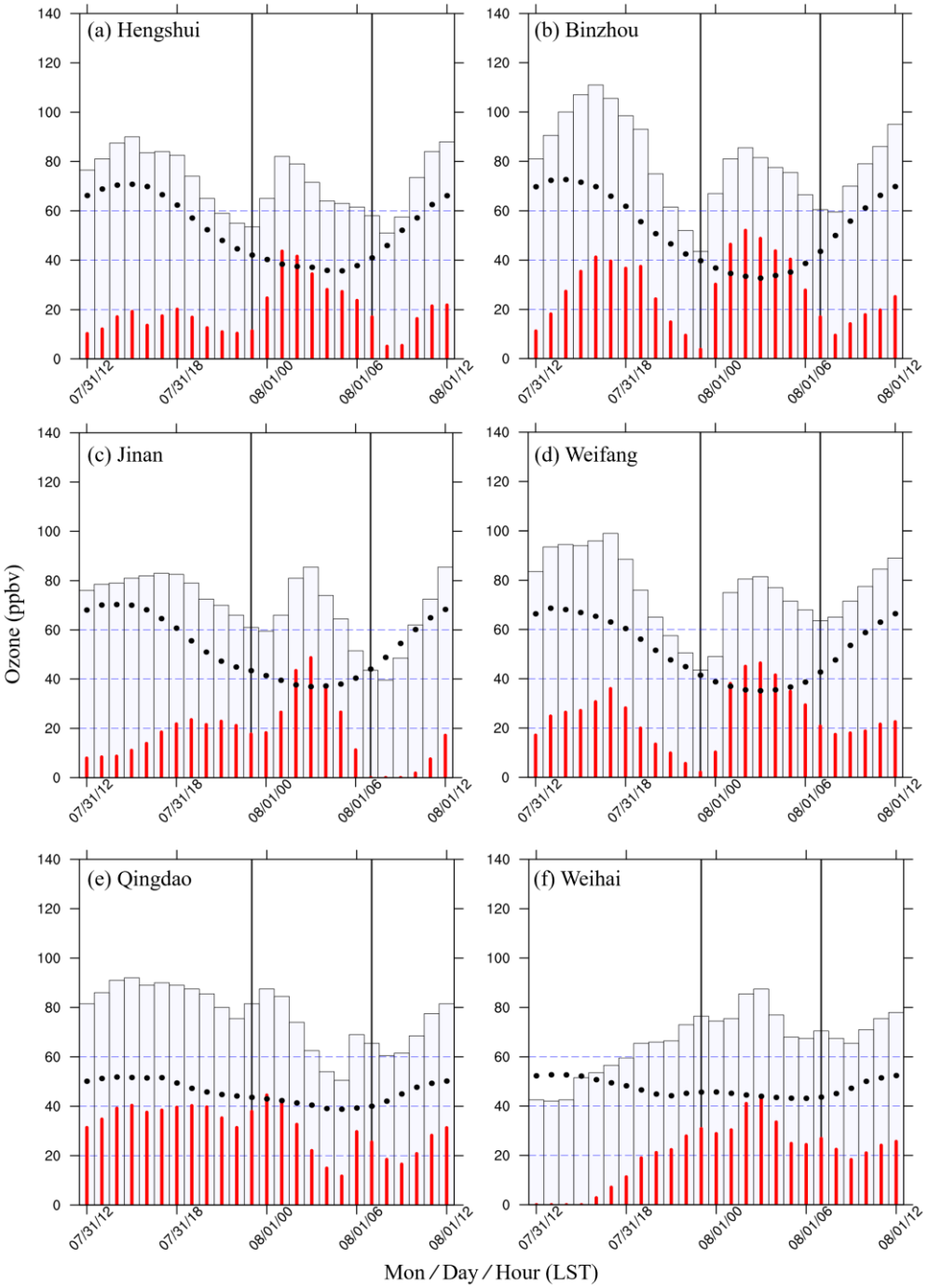

Figure S3: Temporal variation in surface ozone concentrations (purple bars; unit: ppbv) from 12:00 LST (local standard time) on 31 July to 12:00 LST on 01 August 2021 in cities Hengshui, Binzhou, Jinan, Weifang, Qingdao, and Weihai. The black solid dots represent the mean ozone concentrations at each hour during the 2021 summer, and the red lines represent the departure of hourly ozone concentrations from the mean ozone concentrations.

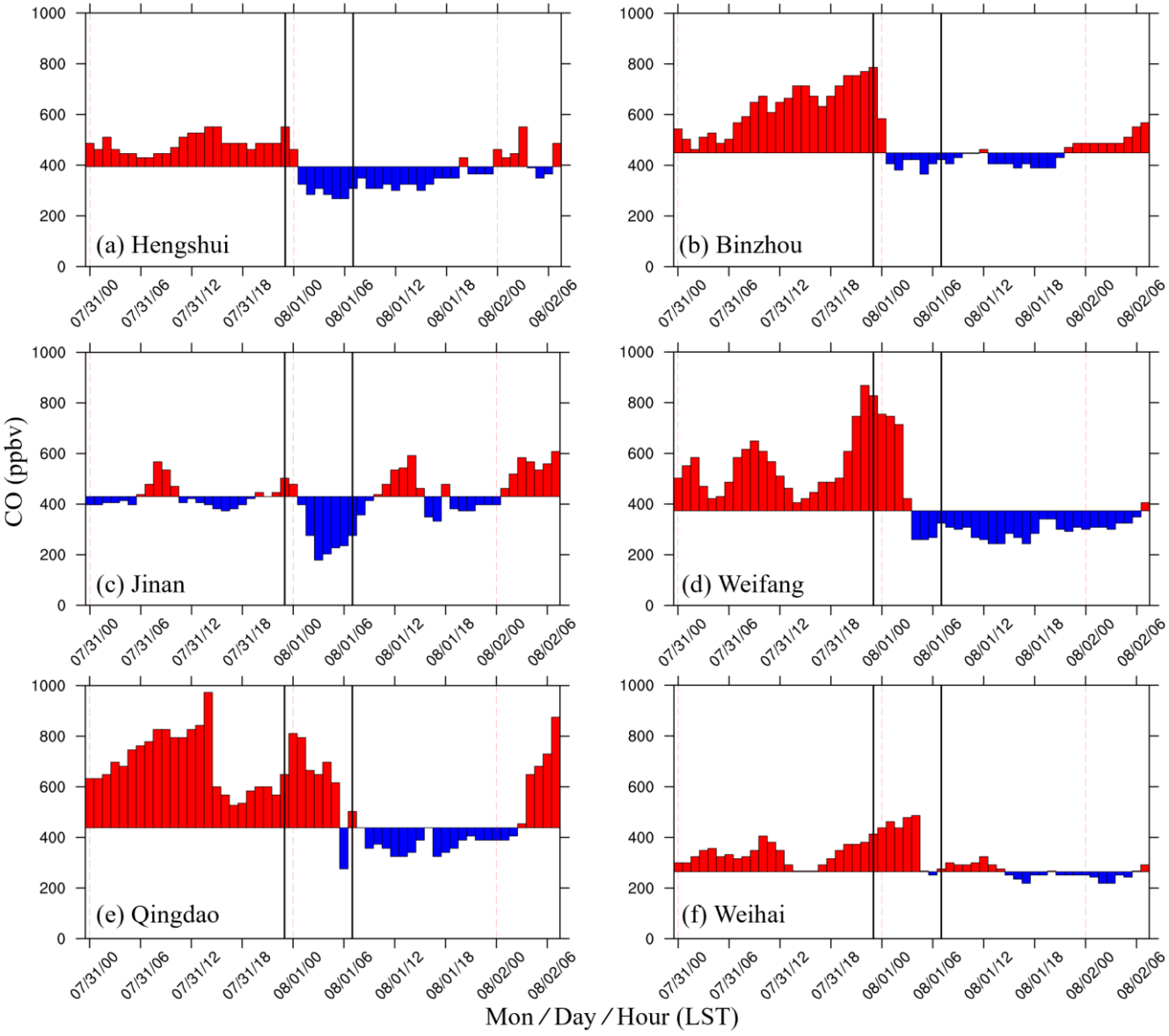

Figure S4: Same as Fig. S2, but for surface carbon monoxide (CO) concentrations from 31 July to 02 August 2021.

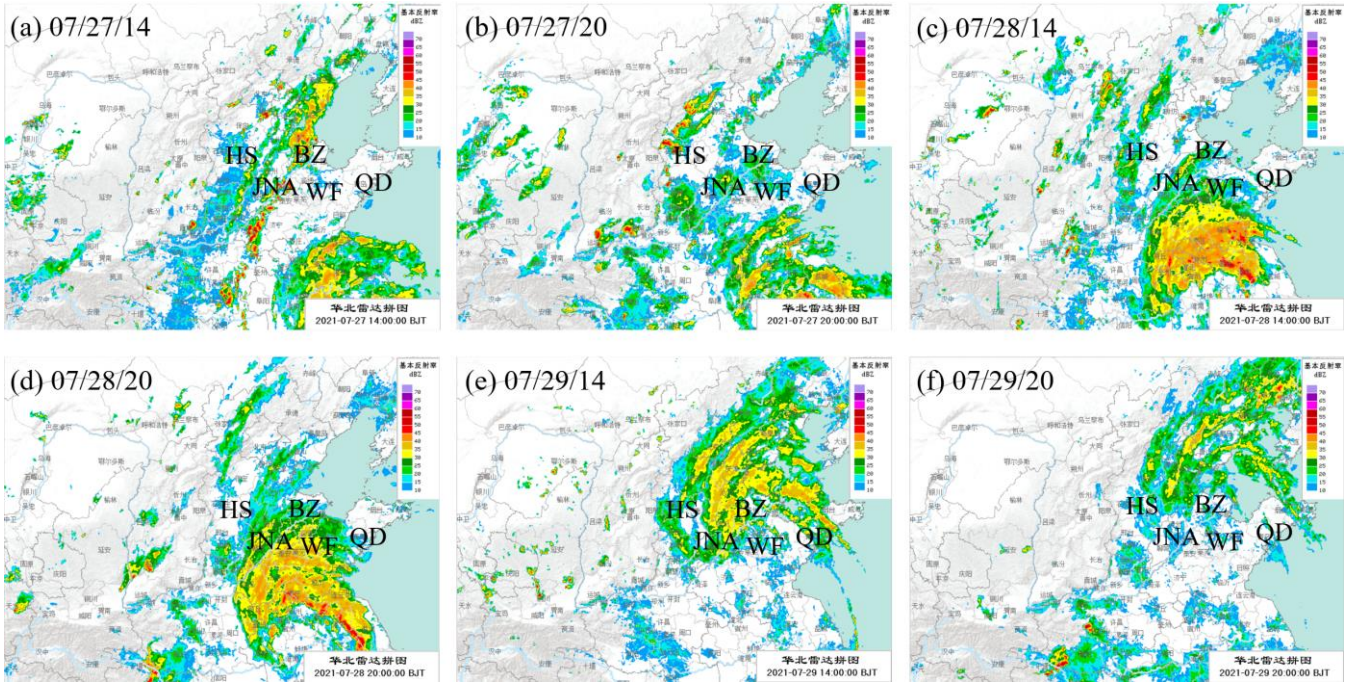

Figure S5: Radar reflectivity maps of the typhoon In-fa over the NCP for different times at (a) 14:00 LST on 27 July, (b) 20:00 LST on 27 July, (c) 14:00 LST on 28 July, (d) 20:00 LST on 28 July, (e) 14:00 LST on 29 July and (f) 20:00 LST on 29 July 2021.

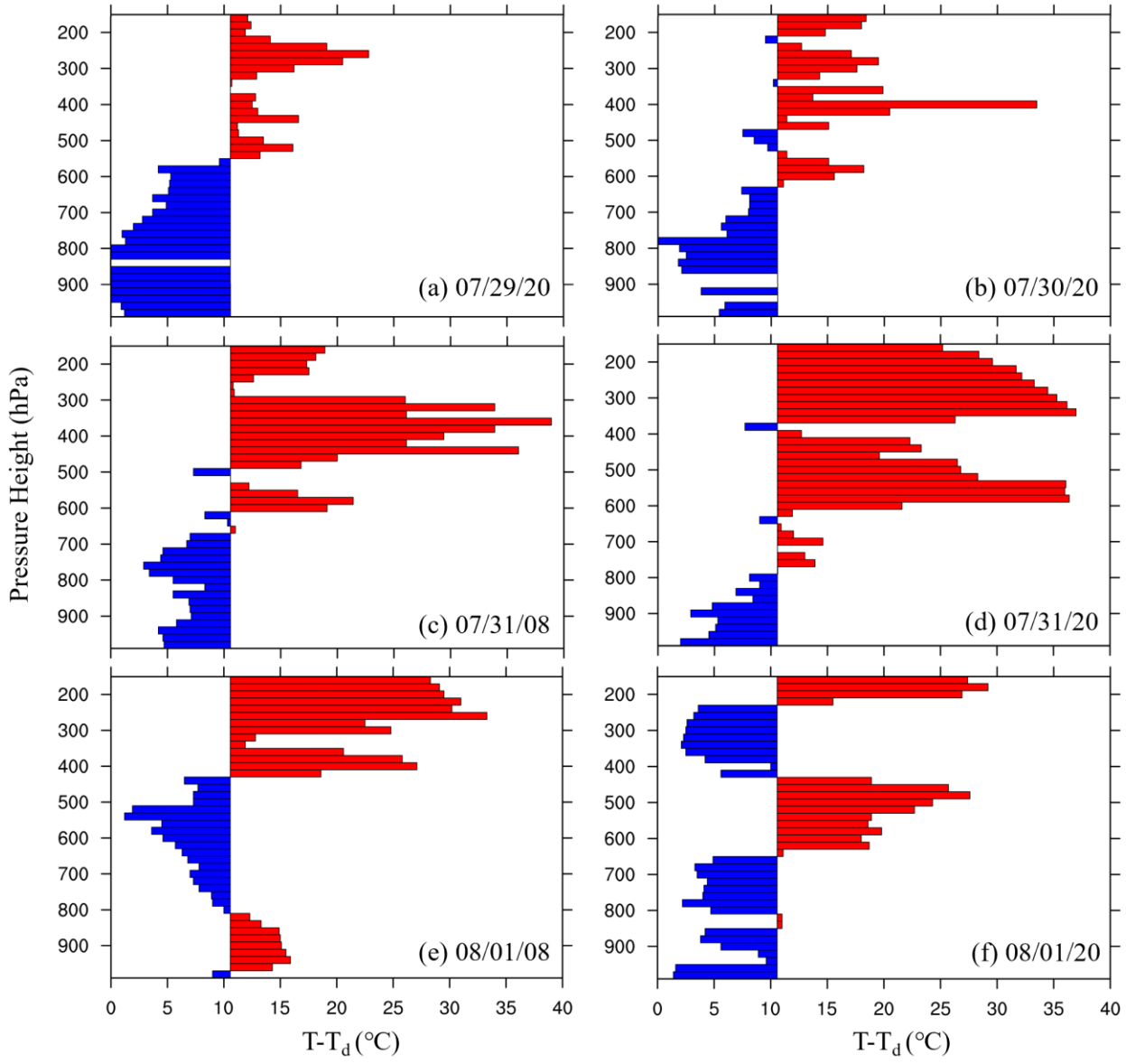

Figure S6: Profiles of dewpoint depressions (T-T_d, unit: ℃) from Qingdao radiosonde observations at (a) 20:00 LST on 29 July, (b) 20:00 LST on 30 July, (c) 08:00 LST, (d) 20:00 LST on 31 July, (e) 08:00 LST 01 and (f) 20:00 LST on 1 August 2021. The 10-day averaged dewpoint depressions between the surface and 700 hPa are used as the baseline, and positive (negative) departure from the 10-day averaged value is shown in red (blue) color.

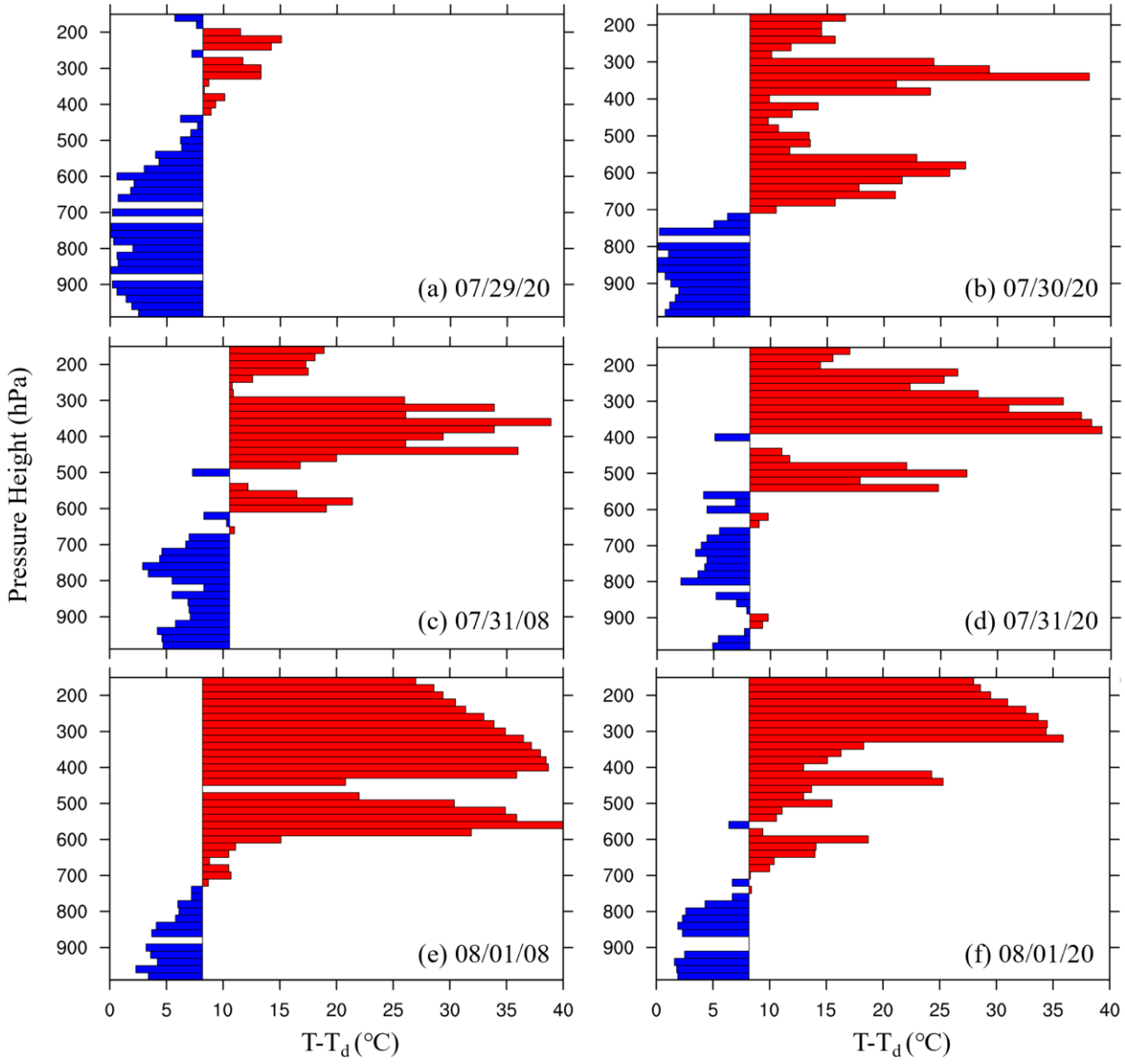

Figure S7: Same as Fig. S4, but for Weihai radiosonde observations.

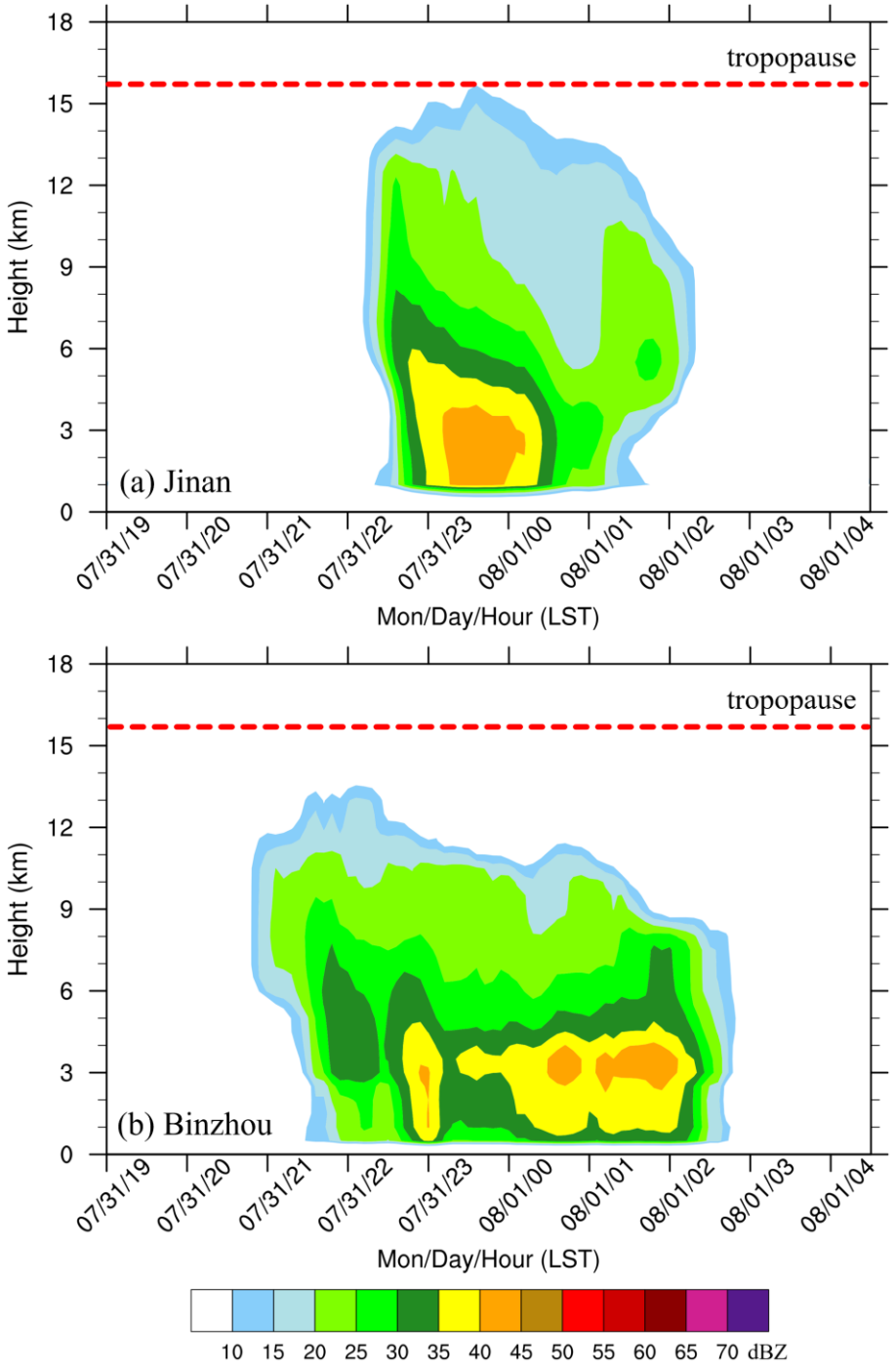

Figure S8: Temporal variations in vertical radar reflectivity profiles over (a) Jinan and (b) Binzhou (shaded; dBZ). The red dashes line represents the thermal tropopause height inferred from the radiosonde observations in Jinan at 20:00 LST on 31 July 2021.

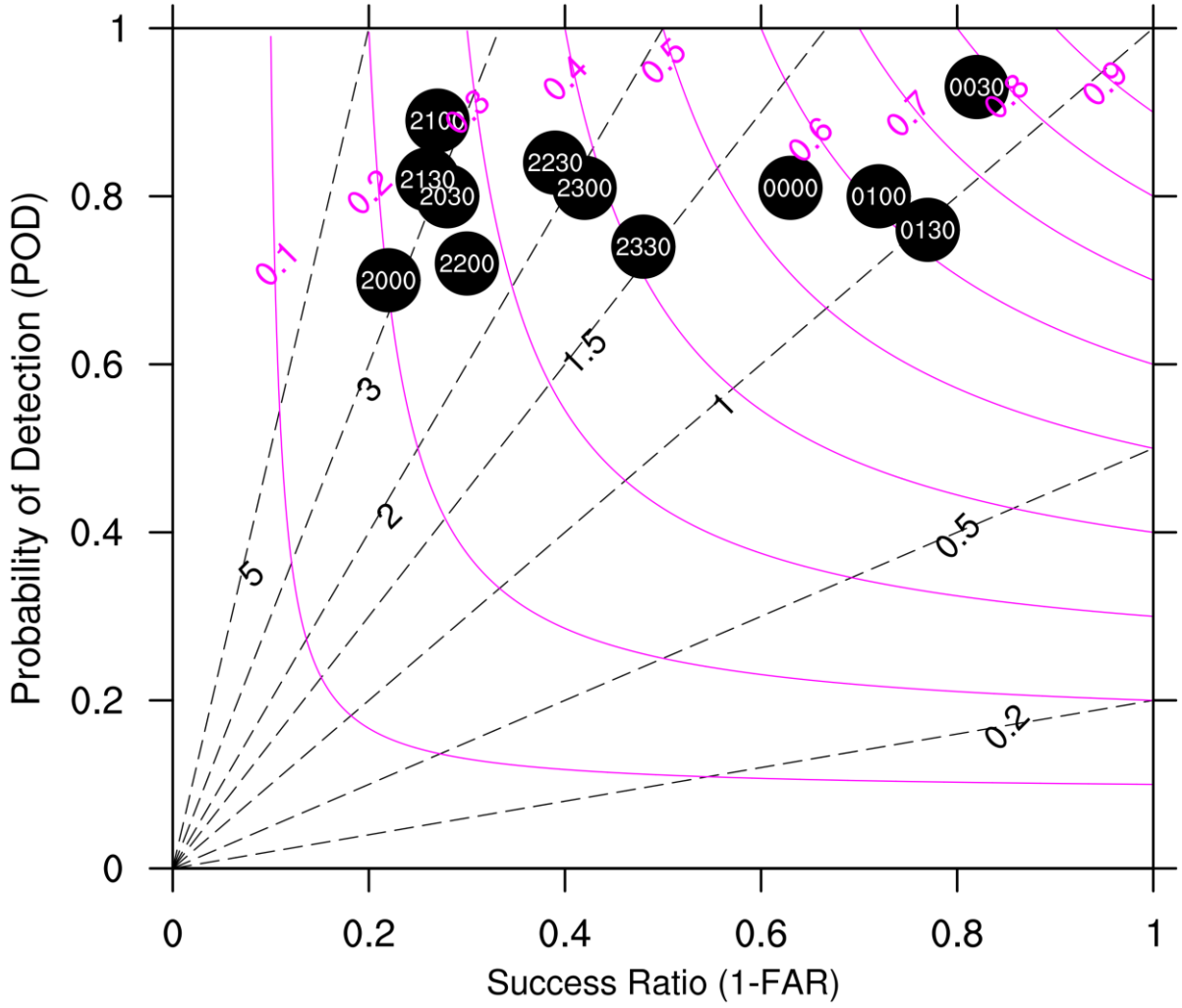

Figure S9: Performance diagram for each 30-min simulations with thresholds of 30 dBZ radar reflectivity threshold stating from 20:00 LST on 31 July 2021. The results are shown for a neighbourhood radius of 20 km. In the performance diagrams, the horizontal axis represents the success ratio (SR), the vertical axis represents the probability of detection (POD), the magenta lines represent the critical success index (CSI), the black dashed lines represent the frequency bias (FB), and the numbers inside the solid circles represent the simulation time.